International Research Journal of Natural and Applied Sciences
ISSN: (2349-4077)
Impact Factor 7.032 Volume 12, Issue 04, April 2025
Website- www.aarf.asia, Email : editor@aarf.asia , editoraarf@gmail.com
Association of Academic Researchers and Faculties (AARF)

Development and Optimization of Albumin Microspheres for Controlled Delivery of pBR322 Plasmid DNA to Tumor Tissue: A Biopolymer-Based Gene Delivery Approach

Suresh Sakhiya[1]*, Dr. Nishant Oza[2]

1. Assistant Professor, Shree H. N. Shukla Institute of Pharmaceutical Education & Research, Rajkot-360005, Affiliated to Gujarat Technological University, Gujarat, India.
2. Dr. Nishant Oza, Controller of Examination, Swarnim Gujarat Sports University, Desar, Gujarat, India

***Correspondence to:**
Suresh Sakhiya, Ph.D. Scholar, C.U. Shah University,
Assistant Professor, Shree H. N. Shukla Institute of Pharmaceutical Education & Research-Rajkot-360005, Gujarat (India).
Email: suresh.sakhiya@gmail.com.

Abstract

Recent studies indicate that genetically driven diseases are more prevalent than previously assumed, with cancer being a prominent example. Traditional therapies have shown limited effectiveness in addressing such complex conditions, making gene therapy an increasingly accepted alternative. Effective gene therapy requires robust gene delivery methods capable of introducing therapeutic DNA into target cells without degradation. While several delivery techniques exist, many fail to achieve the desired precision and efficacy. Among these approaches, microspheres have shown significant promise. This study focuses on developing albumin-based microspheres for the microencapsulation and delivery of the pBR322 plasmid vector, a reliable carrier for gene therapy. Controlled release systems utilizing biocompatible and biodegradable polymers like albumin offer numerous advantages over conventional delivery methods. Albumin, a natural biopolymer, is not only biodegradable but also preferentially absorbed by tumor tissues, making it an ideal choice for formulating targeted gene delivery systems. Using the solvent evaporation technique, pBR322-loaded albumin microspheres were prepared and optimized for targeted tumor gene delivery. Different concentrations of albumin and DNA were evaluated to identify the combination that maximizes DNA encapsulation and controlled release. The study demonstrates that this could play a significant role in the future of targeted gene therapy for cancer.

Keywords: Gene Therapy, Gene Delivery, Microspheres, Albumin

Introduction

Cancer, a diverse group of diseases marked by uncontrolled cell growth and spread due to genetic and epigenetic alterations, is a leading cause of global morbidity and mortality. This introduction explores the multifaceted nature of cancer, encompassing its signs and symptoms, global prevalence, underlying pathophysiology, diagnostic modalities, treatment strategies, and the emergence of targeted therapies. Furthermore, it delves into the concepts of tumors, gene therapy, microspheres, albumin microspheres, and the specific gene vector pBR322, setting the stage for the research presented.

Early-stage cancers often lack specific symptoms, making detection challenging. General symptoms include fatigue, weight loss, fever, and night sweats. Localized symptoms vary depending on the cancer type and location, such as coughing in lung cancer, breast lumps, or bowel changes in colorectal cancer. Advanced cancer can lead to systemic complications. Early detection through awareness and screening significantly improves prognosis (1).

Globally, cancer caused approximately 10 million deaths out of 19.3 million new cases in 2020. Incidence varies geographically due to genetics, environment, lifestyle, and healthcare access. Lung, breast, colorectal, and prostate cancers are most common, with stomach, liver, and esophageal cancers contributing significantly to mortality, particularly in lower-income countries. Lifestyle factors and infectious agents also play a crucial role in cancer risk. Prevention, education, and equitable access to care are vital in reducing the global cancer burden.

The pathophysiology of cancer involves genetic, epigenetic, and microenvironmental changes that enable cells to bypass normal regulatory mechanisms. Key "hallmarks of cancer" include sustained proliferation, evasion of growth suppressors, resistance to apoptosis, replicative immortality, angiogenesis, and metastasis. Molecularly, mutations in oncogenes, tumor suppressor genes, and DNA repair genes drive cancer development. The tumor microenvironment (TME) and metastasis are critical aspects of cancer progression.

Accurate and timely diagnosis is essential, involving clinical evaluation, imaging (X-rays, CT, MRI, PET), laboratory tests, and histopathology. Advanced techniques like liquid biopsies and next-generation sequencing (NGS) are improving early detection and personalized treatment strategies.

Cancer treatment is multidisciplinary, including surgery, radiation therapy, chemotherapy, immunotherapy, and targeted therapies. Precision oncology, guided by molecular profiling, tailors treatment to individual tumor characteristics.

Tumors, abnormal cell growths, can be benign or malignant, with malignant tumors (cancers) posing the greatest threat due to their invasive and metastatic potential. Tumor symptoms vary by type and location, ranging from localized effects like headaches or bowel issues to systemic symptoms such as weight loss and fatigue (2). Prevalence and risk factors mirror those of cancer. Tumor pathophysiology involves disruptions in cellular processes, driven by genetic, epigenetic, and environmental factors, exhibiting the hallmarks of cancer. Diagnosis involves imaging, biomarkers, liquid biopsies, and histopathology. Treatment options are similar to those for cancer, including surgery, radiation, chemotherapy, and targeted therapies.

Gene therapy involves introducing, altering, or removing genes to treat or prevent disease by targeting the genetic basis of the condition. It is classified into germ line (heritable) and somatic (non-heritable) therapy. Approaches include gene replacement, repair, silencing, and

epigenetic modulation. Gene transfer methods can be viral (retroviruses, adenoviruses, adeno-associated viruses) or non-viral (physical methods like electroporation and gene gun, biochemical methods like lipoplexes and dendrimers).

Microspheres are small spherical particles used as carriers for therapeutic agents, offering targeted and sustained drug delivery, particularly for anti-cancer drugs. Biodegradable microspheres can be made from natural polymers like albumin and polysaccharides or synthetic polymers like PLA, PGA, and PLGA. Preparation methods include emulsion solvent evaporation, solvent extraction, cross-linking, precipitation, freeze drying, spray drying, melt method, and supercritical fluid techniques (3).

Albumin, a natural protein, is an ideal material for microspheres due to its biocompatibility and non-toxic nature, offering controlled release and targeted drug localization, especially for tumor therapy (4). Tumor cells exhibit preferential uptake of albumin, enhancing targeted drug delivery. Albumin microspheres can encapsulate various therapeutic agents and can be modified to enhance targeting.

pBR322, an early and influential artificial plasmid, is a key tool in genetic engineering. This 4,361 base pair circular DNA plasmid contains a replication origin and antibiotic resistance genes for ampicillin and tetracycline, along with multiple restriction sites (5). It has been instrumental in gene cloning and molecular biology research. This study aims to utilize albumin microspheres for the targeted delivery of the pBR322 plasmid vector for tumor treatment, addressing limitations in current gene delivery systems by leveraging albumin's properties and microsphere technology for enhanced efficacy and safety.

This research details the comprehensive materials and methodologies employed for the isolation and characterization of plasmid DNA, and subsequently, the formulation and evaluation of albumin microspheres designed for its delivery. The experimental workflow encompasses standard molecular biology techniques, pharmaceutical formulation methods, and in vitro cell culture studies.

3.1. Isolation of Plasmid DNA

The isolation of plasmid DNA was performed using the alkaline lysis method with lysozyme, a widely adopted technique for obtaining relatively pure plasmid DNA from bacterial cultures (6).

3.1.1. Materials

A diverse array of chemicals and reagents were essential for this process. These included standard laboratory chemicals such as Glucose, Sucrose, Tris-chloride, EDTA, NaOH, SDS, NaCl, Potassium acetate, Glacial acetic acid, Phenol, Chloroform, Isopropanol, and Ethanol, sourced from various suppliers. Specialized biological reagents like Lysozyme, TE buffer, Agarose, Ethidium Bromide, Bromophenol Blue, Plasmid DNA (specifically pBR322), and TAE Buffer were also utilized (7). For the subsequent steps involving microsphere preparation and cell culture, Egg Albumin, Tween-80, Hydrochloric Acid, Cottonseed Oil, Diethyl Ether, Human adenocarcinoma cell line (MCF-7), DMEM supplemented with FBS, Penicillin/Streptomycin, Trypsin-EDTA solution, Phosphate-buffered saline (PBS), MTT reagent, Lipofectamine, and DAPI stain were required.

Several key reagents were prepared in the laboratory according to established protocols to ensure consistency and efficacy. These included 0.5 M EDTA (pH 8.0) for chelating divalent

cations that can degrade DNA, 10% (v/v) Glycerol for cryoprotection if storing bacterial stocks, LB (Luria-Bertani Medium) for bacterial growth, 10 mg/ml Lysozyme solution for enzymatic digestion of bacterial cell walls, 5 M NaCl for salt treatment, 20% (w/v) SDS for cell lysis and protein denaturation, STE Buffer (10 mM Tris-Cl pH 8.0, 0.1 M NaCl, 1 mM EDTA pH 8.0) for resuspension, TE Buffer (100 mM Tris-Cl, 10 mM EDTA pH 8.0) for DNA storage, 1 M Tris-Cl adjusted to specific pH values (7.4, 7.6, or 8.0) for buffering, and 50 mM Tris-Cl with 10% (w/v) Sucrose (pH 8.0) for preparing spheroplasts (8).

A range of standard laboratory instruments facilitated the isolation process. These included an Autoclave for sterilization, Vortex Mixer for vigorous mixing, Cooling Centrifuge for cell pelleting and DNA precipitation, Hot Air Oven for drying, Laminar Airflow Cabinet for aseptic work, Horizontal Electrophoresis Unit for DNA separation, Eppendorf Pipettes for accurate liquid handling, Gel Documentation System for visualizing and photographing DNA gels, UV Transilluminator for visualizing DNA stained with ethidium bromide, Sonicator for cell disruption (though not explicitly used in this alkaline lysis protocol but listed), Magnetic Stirrer for mixing, Dissolution Apparatus for release studies, UV Spectrophotometer for DNA quantification, Cell culture incubator and CO_2 incubator for cell line studies, Fluorescence microscope for visualizing cell uptake, and ELISA reader for cytotoxicity assays.

3.1.3. Method: Isolation of Plasmid DNA by Alkaline Lysis with Lysozyme

The isolation protocol involved several critical steps. First, a single colony of transformed bacteria containing the plasmid was cultured overnight in LB broth with appropriate antibiotics to amplify the plasmid. A 50 ml aliquot of this culture was harvested by centrifugation to obtain a bacterial pellet. This pellet was then sequentially resuspended in ice-cold STE buffer and GTE solution. Lysozyme was added and incubated on ice to partially digest the bacterial cell walls. Subsequently, a 10% SDS solution was added to lyse the cells and denature proteins, followed immediately by the addition of 5 M NaCl to a final concentration of 1 M to precipitate chromosomal DNA and cellular debris. This mixture was incubated on ice, followed by the addition of an ice-cold potassium acetate/acetic acid solution to neutralize the alkaline conditions and enhance precipitation (9).

The clarified lysate, containing the plasmid DNA in the aqueous phase, was then subjected to sequential extractions with phenol: chloroform and chloroform to remove residual proteins and cellular contaminants. The aqueous phase was transferred to a new tube, and DNA was precipitated by adding two volumes of room temperature ethanol. The precipitated DNA was recovered by centrifugation, washed with 70% ethanol to remove salts, and air-dried. Finally, the DNA pellet was dissolved in TE buffer (pH 8.0). The concentration and purity of the isolated plasmid DNA were determined by measuring absorbance at 260 nm and calculating the A260:A280 ratio using a UV spectrophotometer.

3.2. Agarose Gel Electrophoresis

Agarose gel electrophoresis was employed to analyze the isolated plasmid DNA, verify its integrity, and separate it from potential contaminants.

3.2.1. Method for Agarose Gel Electrophoresis

The procedure involved preparing a 1% (w/v) agarose gel by dissolving agarose powder in TAE (Tris-acetate-EDTA) buffer. Ethidium bromide was added to the melted agarose solution to a final concentration of 0.5 µg/ml for DNA visualization under UV light. The cooled agarose solution was poured onto a gel casting platform, and a comb was inserted to create wells. After

the gel solidified, it was placed in an electrophoresis tank filled with TAE buffer. DNA samples, mixed with a 10× loading buffer containing a dense substance and tracking dyes, were loaded into the wells. A DNA molecular weight marker was also loaded as a reference. An electric field was applied, causing the negatively charged DNA molecules to migrate towards the positive electrode (anode). The electrophoresis was continued until the tracking dye reached a sufficient distance(10). The gel was then visualized under a UV transilluminator, and images were captured using a gel documentation system.

3.3. DNA Elution

This method was used to recover purified plasmid DNA directly from the agarose gel after electrophoresis, specifically the band corresponding to the pBR322 plasmid (11).

The target DNA band was carefully excised from the agarose gel using a clean scalpel, minimizing UV exposure by using long-wave UV light. A DNA standard ladder run alongside allowed for estimating the size and concentration of the excised DNA band by comparison. The excised gel fragment was placed on parafilm, and gentle pressure was applied to extrude the DNA along with buffer droplets. These droplets were collected, diluted with sterile TE buffer, and further purified using phenol: chloroform extraction and ethanol precipitation, following the protocol for DNA purification and quantification (12).

3.4. DNA Purification and Quantification

The concentration and purity of the isolated and eluted double-stranded DNA (dsDNA) were determined using UV-Visible spectrophotometry, leveraging the principle that DNA absorbs UV light at 260 nm.

Principle: DNA quantification relies on the direct proportionality between DNA concentration and absorbance at 260 nm. Purity is assessed by the A260:A280 ratio; a ratio near 1.8 indicates pure dsDNA, while deviations suggest protein or RNA contamination. The concentration was calculated using the formula: Concentration (µg/mL) = Absorbance at 260 nm × dilution factor × 50, where 50 is the conversion factor for dsDNA.

3.4.1. Procedure: A diluted aliquot of the DNA sample in TE buffer was prepared. A clean quartz cuvette was used for measurement. The UV-Vis spectrophotometer was warmed up and zeroed using TE buffer as a blank. The absorbance of the DNA sample was then measured at 260 nm and 280 nm. The concentration was calculated using the formula, accounting for the dilution factor. The A260:A280 ratio was calculated to assess purity, comparing it to the ideal value of 1.8 for pure dsDNA (13).

3.5. Preparation of Microspheres

Albumin microspheres, both placebo and DNA-loaded, were prepared using the solvent evaporation technique (14).

3.5.1. Method

3.5.1.1. Preparation of Albumin Microspheres as Placebo: A 10% aqueous solution of egg albumin was added dropwise into cottonseed oil at room temperature with vigorous stirring to form a water-in-oil (W/O) emulsion. This emulsion was then added dropwise into preheated cottonseed oil (90°C) with continued stirring at an intermediate speed to stabilize the emulsion and solidify the albumin. The suspension was left undisturbed for 24 hours for complete

hardening. The supernatant oil was decanted, and the microspheres were washed three times with diethyl ether to remove residual oil (15). The microspheres were resuspended in diethyl ether and stored at 4°C. Nine batches of placebo microspheres were prepared.

3.5.1.2. Preparation of DNA-Loaded Albumin Microspheres: A 10% aqueous solution of egg albumin containing 0.02% (w/v) pBR322 plasmid DNA was added dropwise into cottonseed oil at room temperature with high-speed stirring to form a W/O emulsion. This emulsion was then added dropwise into preheated cottonseed oil (90°C) and stirred at an intermediate speed for 5 minutes to facilitate albumin solidification and DNA encapsulation. The suspension was left for 24 hours for hardening. The oil was decanted, and the DNA-loaded microspheres were washed three times with diethyl ether. The microspheres were resuspended in diethyl ether and stored at 4°C (16). Nine batches of DNA-loaded microspheres were prepared with varying albumin and DNA concentrations.

3.6. Evaluation of Microspheres

The prepared microspheres were evaluated for their physicochemical characteristics.

3.6.1. Determination of Average Diameter of Microspheres: The average diameter was determined using optical microscopy with a calibrated stage micrometer. The diameters of at least 100 microspheres per batch were measured.

3.6.1.1. Calibration of the Stage Micrometer: The eyepiece micrometer was calibrated against a stage micrometer at a specific magnification. Observations of aligning divisions on both micrometers allowed for calculating the size of one eyepiece division (determined to be 2.67 µm).

3.6.1.2. Determination of Mean Diameter: The mean diameter was calculated using a formula suitable for grouped data: Mean Diameter = $(\Sigma (f \times a)) / \Sigma f$, where 'f' is the frequency and 'a' is the mid-value of the size range (17).

3.6.1.3. Determination of Standard Deviation: The standard deviation (SD) of particle sizes was calculated using the formula: $SD = \sqrt{[\Sigma (f \times (a - Mean)^2)] / (N - 1)}$, where 'N' is the total frequency. A percentage frequency polygon was plotted to analyze particle size distribution.

3.6.2. Shape: The shape of the microspheres was examined using Scanning Electron Microscopy (SEM) after air-drying and gold coating. SEM analysis confirmed a predominantly spherical shape.

3.6.3. DNA Entrapment Efficiency: The percentage of initially added DNA successfully encapsulated was determined by comparing theoretical and practical yields (18).

3.6.3.1. Theoretical Yield: Calculated assuming complete encapsulation of all added DNA.

3.6.3.2. Practical Yield: Experimentally determined by weighing dried microspheres, extracting encapsulated DNA using an acidic ethanolic solution (5% HCl in 95% ethanol), and quantifying the extracted DNA spectrophotometrically at 260 nm. Entrapment efficiency was calculated as (Practical Yield / Theoretical Yield) × 100%.

3.6.4. In Vitro Dissolution Study: The release of plasmid DNA from DNA-loaded microspheres was assessed in phosphate buffer (pH 7.4) containing 2% Tween-80 (19).

3.6.4.1. Procedure: A weighed number of DNA-loaded microspheres (equivalent to 0.1 µg DNA) was suspended in dissolution medium at 37°C with continuous stirring. Aliquots were withdrawn at intervals, centrifuged, and the supernatant absorbance was measured at 260 nm against a blank. Fresh medium was added back after each sampling (20).

3.6.4.2. Preparation of Phosphate Buffer Solution (pH 7.4): Prepared by mixing 0.2 M monobasic potassium phosphate solution with 0.2 M NaOH solution and adjusting the final volume with distilled water to achieve pH 7.4.

3.7. In Vitro Cell Line Study Method

The biological efficacy of DNA-loaded microspheres was evaluated using MCF-7 human adenocarcinoma cells for transfection efficiency and cytotoxicity (21).

3.7.1. Methodology: MCF-7 cells were seeded in 6-well plates and incubated overnight. Cells were treated with DNA-loaded microspheres at varying DNA equivalent concentrations (5, 10, 15 µg/mL). Lipofectamine-pBR322 complexes served as a positive control, and untreated cells as a negative control. After incubation, cells were washed and fresh medium was added (21).

Transfection Efficiency (Fluorescence Imaging): After 48 hours, cells were stained with DAPI to visualize nuclei and potentially a fluorescent label for the plasmid DNA. Cellular uptake and DNA localization were observed using a fluorescence microscope. Fluorescence intensity was quantified using ImageJ software.

Cytotoxicity (MTT Assay): Cells were incubated with different microsphere concentrations for 48 hours. MTT reagent was added, and viable cells reduced it to formazan crystals, which were dissolved in DMSO. Absorbance was measured at 570 nm using an ELISA reader. Cell viability was calculated as the percentage of absorbance relative to untreated control cells (22).

This section presents the detailed findings derived from the experimental investigations into plasmid DNA isolation, characterization, and the formulation and evaluation of albumin microspheres as a delivery system for the isolated DNA.

4.1. DNA Isolation from *E. coli* pBR322

The process of isolating plasmid DNA from *E. coli* using the alkaline lysis method yielded DNA of notable purity and concentration (23).

4.1.1. Purification

The purity of the isolated plasmid DNA was quantitatively assessed by measuring the absorbance at 260 nm and 280 nm using a UV spectrophotometer. The ratio of these absorbances (A_{260}/A_{280}) is a widely accepted indicator of nucleic acid purity, with a ratio of approximately 1.8 signifying highly pure DNA. As detailed in Table 4, the measured absorbance at 260 nm was 1.66, and the absorbance at 280 nm was 0.98 (24). This resulted in a calculated A_{260}/A_{280} ratio of 1.69. This value, being close to the ideal ratio of 1.8, strongly suggests that the isolated plasmid DNA was of high purity, with minimal contamination from proteins (which absorb strongly at 280 nm) or other cellular components. A ratio lower than 1.6 typically points towards significant RNA contamination, while a ratio above 1.8 could indicate protein contamination. The obtained ratio of 1.69 confirmed that the isolation protocol effectively minimized such contaminants, yielding DNA suitable for downstream applications (25).

Table 4. DNA Purity from *E. coli* pBR322

Absorbance at 260 nm (A_1)	Absorbance at 280 nm (A_2)	A_1/A_2
1.66	0.98	1.69

4.1.2. Quantification

The concentration of the isolated plasmid DNA was determined spectrophotometrically using the established formula: Concentration (µg/mL) = Absorbance at 260 nm × dilution factor × 50. With the measured absorbance at 260 nm being 1.66, and assuming no dilution was applied for this specific measurement (a dilution factor of 1), the concentration of the isolated DNA stock solution was calculated to be 1.66 × 1 × 50 = 83 µg/ml. This concentration indicates a substantial yield of plasmid DNA from the bacterial culture, demonstrating the effectiveness of the optimized alkaline lysis protocol for obtaining a significant quantity of plasmid DNA (26).

4.2. Agarose Gel Electrophoresis

Agarose gel electrophoresis was performed to visually confirm the presence, integrity, and size of the isolated plasmid DNA. The isolated DNA samples were run on a 1% agarose gel prepared with TAE buffer and stained with ethidium bromide for visualization under UV light. Molecular weight markers (DNA ladders) were included to allow for accurate size estimation of the isolated plasmid (27).

Reference bands of known plasmids, pUC18 and pBR322, were included in the gel. The pUC18 reference band (R1) migrated to a position corresponding to approximately 2.65 kilobases (KB), consistent with its known size. The pBR322 reference band (R2), which is the target plasmid for this study, migrated to approximately 4.33 KB, also in agreement with its established molecular weight (28).

The isolated DNA samples, loaded in lanes labeled S1 to S5, showed clear and well-defined bands. Crucially, these sample bands migrated to the same position as the pBR322 reference band (R2), aligning at approximately 4.33 KB (29). The sharpness of the observed bands, without significant smearing, indicated that the isolated plasmid DNA remained largely intact and did not suffer significant degradation during the isolation procedure. Minor variations in the intensity of the bands across samples S1 to S5 were noted, likely reflecting slight differences in the amount of DNA loaded into each well. The characteristic migration of the negatively charged DNA bands towards the positive electrode (anode) further validated the success of the electrophoretic separation and the expected behavior of the isolated nucleic acid. The results from agarose gel electrophoresis definitively confirmed the successful isolation of plasmid DNA with the correct size and good integrity, supporting the reliability of the isolation methodology.

S1 to S5: DNA samples showed clear and distinct bands aligning with the pBR322 reference band at 4.33 KB.

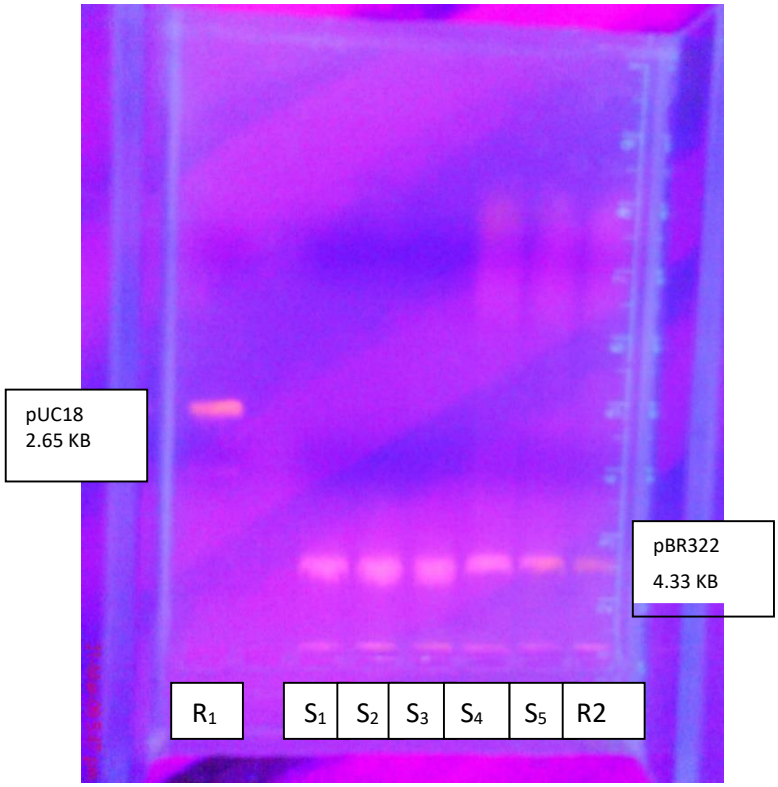

Figure 1. Gel electrophoresis

4.3. DNA Elution

Following agarose gel electrophoresis, the plasmid DNA band corresponding to pBR322 was excised from the gel, and the DNA was eluted and further purified (30). The purity and concentration of this eluted DNA were subsequently assessed.

4.3.1. Purification

The purity of the plasmid DNA eluted from the agarose gel was evaluated using spectrophotometry, measuring absorbance at 260 nm and 280 nm. As shown in Table 5, the absorbance at 260 nm was 4.9, and the absorbance at 280 nm was 2.89. This yielded an A_{260}/A_{280} ratio of 1.70. This ratio is remarkably close to the ideal value of 1.8 for pure double-stranded DNA, indicating that the elution and subsequent purification steps were highly effective in removing agarose residues and other potential contaminants that might have been present in the gel matrix or introduced during the elution process (31). A high purity is essential for ensuring the efficacy of the DNA when encapsulated in microspheres and used in downstream applications like transfection.

Table 5. Purified DNA Elution: Absorbance and Purity

Absorbance at 260 nm (A_1)	Absorbance at 280 nm (A_2)	A_1/A_2 Ratio
4.9	2.89	1.70

4.3.2. Quantification

The concentration of the eluted plasmid DNA was also determined spectrophotometrically. Based on the absorbance of 4.9 at 260 nm and assuming no initial dilution, the concentration was calculated as 4.9 × 1 × 50 = 245 µg/ml. The text also presents data for a further diluted sample where 800 µL of eluted DNA was diluted to a final volume of 1000 µL in TE buffer (a dilution factor of 1.25) (32). For this diluted sample, the measured absorbance at 260 nm was 3.8, and the calculated concentration was stated as 190 µg/ml. While a direct calculation from the provided absorbance and dilution factor (3.8 × 1.25 × 50 = 237.5 µg/mL) shows a slight discrepancy with the reported value of 190 µg/mL, the key finding is that the elution method successfully recovered a substantial amount of purified plasmid DNA.

4.4. Albumin Microsphere

The study involved the preparation and characterization of albumin microspheres, both as a placebo (without DNA) and loaded with the isolated pBR322 plasmid DNA (33).

4.4.1. Albumin Microsphere as a Placebo

Placebo albumin microspheres, formulated using a 10% (w/v) albumin solution without the incorporation of plasmid DNA, were characterized microscopically. Optical microscopy revealed that these microspheres were predominantly spherical in shape and exhibited a high degree of uniformity in their size distribution. Further detailed analysis using Scanning Electron Microscopy (SEM) confirmed their well-defined circular morphology and provided a more precise measurement of their size, indicating a mean particle size (MPS) of approximately 9.2 µm. The consistent spherical shape and uniform size are desirable attributes for drug delivery systems, potentially influencing factors such as flowability and cellular uptake (34).

4.4.2. pBR322 Plasmid-Loaded Albumin Microsphere

Albumin microspheres successfully encapsulated the isolated pBR322 plasmid DNA using the solvent evaporation technique. Similar to the placebo microspheres, the DNA-loaded microspheres were also observed to be predominantly circular in shape. However, the incorporation of plasmid DNA resulted in a slight increase in their mean particle size compared to the placebo microspheres. For microspheres prepared with a 10% (w/v) albumin concentration and a 0.02% (w/v) DNA concentration, the mean particle size was determined to be approximately 13.5 µm. This increase in size is a logical consequence of the physical presence of the plasmid DNA molecules within the albumin matrix during the microsphere formation process (35).

4.5. Shape

Detailed examination of the albumin microspheres using Scanning Electron Microscopy (SEM) provided compelling visual evidence of their morphology. The SEM images consistently demonstrated that the prepared microspheres possessed a predominantly circular or spherical shape across different batches and preparation conditions (36). These morphological characteristics can positively influence the flow properties of the microsphere formulation, their interaction with biological environments and cells, and ultimately, the rate and pattern of drug or DNA release.

4.6. Size

The mean particle size (MPS) of the albumin microspheres was systematically investigated as a function of the albumin concentration used during their preparation. The results clearly indicated that the concentration of the polymer (albumin) played a crucial role in determining the final size of the microspheres (37). Microspheres formulated with a lower albumin concentration of 5% (w/v) exhibited a smaller MPS, ranging from approximately 8.4 µm. As the albumin concentration was increased to 15% (w/v), a significant increase in MPS was observed, reaching approximately 20.8 µm.

4.7. Entrapment Efficiency

The efficiency with which the pBR322 plasmid DNA was successfully encapsulated within the albumin microspheres (Entrapment Efficiency, PE%) was a critical parameter evaluated in this study. The PE% was determined for various formulations prepared with different concentrations of both albumin and the incorporated plasmid DNA (38). The key findings related to entrapment efficiency are summarized in Table 6.

Table 6. Effect of albumin concentration and concentration of DNA incorporated on MPS and PE.

Conc. of Albumin (% w/v)	DNA Conc. (% w/v)	MPS (µm)	OD	PE%
5	0.01	8.3	0.08	40.2
10	0.01	15	0.107	53.5
15	0.01	20.7	0.094	45.8
5	0.02	8	0.119	61
10	0.02	12.8	0.135	68
15	0.02	19.5	0.11	56.5
5	0.05	7.8	0.079	41

10	0.05	12.5	0.109	54.5
15	0.05	19.1	0.096	48

4.8. Effect of Albumin Concentration and Concentration of DNA Incorporated on MPS and PE

Table 6 provides a detailed breakdown of the experimental results, showing the combined effect of varying albumin concentrations and initial DNA concentrations on both the mean particle size (MPS) and the percentage entrapment efficiency (PE%) of the microspheres. The data presented in this table are central to understanding how the formulation parameters influence the physical characteristics and the drug loading capacity of the microspheres (39).

The data in Table 6 show that the mean particle size (MPS) of the microspheres ranged from a minimum of 7.8 µm to a maximum of 20.7 µm across the different formulations. A clear trend of increasing MPS with increasing albumin concentration is evident, regardless of the initial DNA concentration. For instance, at a DNA concentration of 0.01% (w/v), increasing the albumin concentration from 5% to 10% and then to 15% resulted in MPS values of 8.3 µm, 15 µm, and 20.7 µm, respectively. This confirms the significant influence of albumin concentration on particle size, as discussed earlier.

The percentage entrapment efficiency (PE%) of the plasmid DNA ranged from a low of 40.2% to a high of 68.0%. Analysis of the data reveals that both albumin and DNA concentrations impact the PE%. Generally, increasing the concentration of either albumin or DNA tends to improve the entrapment efficiency up to a certain point. For example, at a 10% (w/v) albumin concentration, increasing the DNA concentration from 0.01% to 0.02% resulted in an increase in PE% from 53.5% to 68%. However, further increasing the DNA concentration to 0.05% at the same albumin concentration led to a slight decrease in PE% to 54.5%, suggesting potential saturation or limitations in the encapsulation process at higher DNA loads (40). Similarly, for a fixed DNA concentration (e.g., 0.02% w/v), increasing the albumin concentration from 5% to 10% increased the PE% from 61% to 68%, but a further increase to 15% albumin resulted in a decrease to 56.5%. This indicates that there might be an optimal combination of albumin and DNA concentrations for achieving maximum entrapment efficiency.

4.8.1. Effect of Albumin Concentration on Mean Particle Size

Reiterating the findings from Table 6 the effect of albumin concentration on the mean particle size (MPS) was consistently observed. At the lowest albumin concentration of 5% (w/v), the MPS values were in the range of 7.8 µm to 8.3 µm across the different DNA concentrations. Increasing the albumin concentration to 10% (w/v) led to a notable increase in MPS, with values ranging from 12.5 µm to 15.0 µm. At the highest albumin concentration of 15% (w/v), the microspheres were significantly larger, with MPS values between 19.1 µm and 20.7 µm. This strong positive correlation between albumin concentration and MPS is a critical factor in controlling the physical dimensions of the microspheres, which can in turn influence their behavior in biological systems and their suitability for specific routes of administration (41). The higher viscosity of the more concentrated albumin solutions is the primary factor driving the formation of larger droplets during emulsification, leading to larger solidified microspheres.

4.8.2. Effect of Albumin Concentration on DNA Entrapment Efficiency

The influence of albumin concentration on the DNA entrapment efficiency (PE%) was also clearly demonstrated. The results, as presented in Table 6 indicate that increasing the albumin concentration generally improved the PE% up to a certain point. At a 5% (w/v) albumin concentration, the PE% varied between 40.2% and 61.0% depending on the DNA concentration. A significant enhancement in entrapment was observed when the albumin concentration was increased to 10% (w/v), with PE% values reaching up to 68.0% (at 0.02% DNA). However, a further increase in albumin concentration to 15% (w/v) resulted in a slight decrease in PE%, with values ranging from 45.8% to 56.5%. This suggests that while a higher albumin concentration provides more matrix for encapsulation, excessive viscosity or other factors at very high concentrations might negatively impact the efficiency of DNA incorporation (42). The optimal albumin concentration for maximizing DNA entrapment appears to be around 10% (w/v) under the tested conditions.

4.9. In vitro dissolution study

An in vitro dissolution study was conducted to evaluate the release profile of the encapsulated plasmid DNA from the albumin microspheres over time. The study was performed in phosphate buffer (pH 7.4) containing 2% Tween-80 at 37°C to mimic physiological conditions and enhance the solubility of released components (43).

The cumulative DNA release data obtained from this study are presented in Table 7 shows the amount of DNA released and the corresponding cumulative percentage release at predetermined time points over a total duration of 100 hours. The data clearly indicate a sustained release of DNA from the albumin microspheres. For example, at 20 hours, the cumulative percentage release was approximately 58.2%, and this increased gradually over time, reaching around 80.8% at 100 hours. This sustained release profile is a desirable characteristic for a drug delivery system, as it can potentially maintain therapeutic levels of the encapsulated DNA over an extended period, reducing the frequency of administration (44).

Table 7. In vitro study data

Time (hours)	Amount of DNA Released (µg/ml)	Percentage Release (%)	Cumulative Percentage Release (%)
0	0	0	0
20	0.68	59	58.2
40	0.75	64	63.1
60	0.88	73	73.8
80	0.93	79	78.9
100	0.96	81	80.8

4.10. Results of model fitting batch

To gain a deeper understanding of the mechanism governing DNA release from the albumin microspheres, the in vitro dissolution data were fitted to various mathematical models commonly used to describe drug release kinetics from pharmaceutical formulations. The models tested included Korsmeyer-Peppas, Higuchi, Hixson-Crowell, Weibull, First Order, and Zero Order models. The goodness of fit for each model was assessed based on statistical parameters such as the sum of squared residuals (SSR), F-statistic (F), correlation coefficient (r), and the coefficient of determination (R^2) (45).

Table 8 presents the results of this model fitting analysis. By comparing the R^2 values, which represent the proportion of the variance in the dependent variable (cumulative DNA release) that is predictable from the independent variable (time) based on the model, the best-fitting model can be identified. The Korsmeyer-Peppas model exhibited the highest R^2 value of 0.9723 and a high correlation coefficient (r) of 0.9835. This indicates that the Korsmeyer-Peppas model provides the most accurate description of the DNA release kinetics from the albumin microspheres among the models tested. The Higuchi model also showed a reasonably good fit, with an R^2 value of 0.9212, further supporting a diffusion-controlled release mechanism. In contrast, models like Hixson-Crowell and Zero Order kinetics showed significantly lower R^2 values (0.8256 and 0.7012, respectively), suggesting they were less suitable for describing the observed release profile (46).

The Korsmeyer-Peppas model includes a diffusional exponent 'n', which provides insights into the release mechanism. For this study, the calculated diffusional exponent (n) from the Korsmeyer-Peppas model was 0.2287. For spherical matrices, an 'n' value less than 0.45 is characteristic of Fickian diffusion, where the release is primarily driven by the concentration gradient of the drug within the matrix. The obtained 'n' value of 0.2287, being well below 0.45, strongly suggests that the release of plasmid DNA from the albumin microspheres is predominantly governed by Fickian diffusion. This implies that the rate of DNA release is controlled by its diffusion through the swollen albumin matrix as the dissolution medium penetrates the microspheres.

Table 8. Model Fitting Results for DNA Release Kinetics from Albumin Microspheres

Parameters	Korsmeyer	Higuchi	Hix-Cro.	Weibull	First Order	Zero Order
SSR	11.089	348.923	998.41	14.123	899.12	1355.42
F	3.4601	87.123	248.72	4.6823	222.89	341.12
r	0.9835	0.9587	0.9178	0.9812	-0.9453	0.8356
R^2	0.9723	0.9212	0.8256	0.9654	0.8851	0.7012
b	0.2287	1.0452	0.0004	0.451	-0.0002	0.0113
a	-0.9214	9.105	0.4598	-1.4235	4.2987	25.1
n (Korsmeyer)	0.2287	-	-	-	-	-

4.11. In-vitro cell line study

To evaluate the biological performance of the pBR322 plasmid DNA-loaded albumin microspheres, an in vitro study was conducted using the MCF-7 human adenocarcinoma cell line. This study assessed both the ability of the microspheres to deliver the plasmid DNA into the cells (transfection efficiency) and their potential toxicity to the cells (cytotoxicity) (47).

4.11.1. Transfection Efficiency

The transfection efficiency was quantified by measuring the fluorescence intensity within the MCF-7 cells after treatment with the DNA-loaded albumin microspheres at different DNA equivalent concentrations (5, 10, and 15 µg/mL). Higher fluorescence intensity correlates with greater uptake and expression of the delivered plasmid DNA (assuming the plasmid contains a fluorescent reporter gene or is detected via fluorescence). As shown in Table 9, the transfection efficiency varied with the concentration of the microspheres. The highest transfection efficiency, indicated by 65% relative fluorescence intensity, was achieved at a microsphere concentration equivalent to 10 µg/mL of DNA (48). At lower concentrations (5 µg/mL), the efficiency was lower (35%), and surprisingly, at a higher concentration (15 µg/mL), the efficiency decreased to 50%. This suggests the existence of an optimal concentration for effective transfection. The positive control, using Lipofectamine (a commercially available and efficient transfection reagent) complexed with pBR322, showed the highest transfection efficiency of 85%, serving as a benchmark. The negative control, untreated cells, exhibited a very low background fluorescence of 5%. The observed decrease in transfection efficiency at the highest microsphere concentration might be attributed to potential aggregation of the microspheres at higher concentrations, which could hinder their effective uptake by the cells (49). The results indicate that while not as efficient as Lipofectamine, the albumin microspheres are capable of delivering plasmid DNA into MCF-7 cells, with an optimal concentration identified at 10 µg/ml.

Table 9. Transfection Efficiency

Concentration (µg/mL)	Fluorescence Intensity (%)
5	35
10	65
15	50
Positive Control	85
Negative Control	5

4.11.2. Cytotoxicity Results (MTT Assay)

The potential cytotoxic effects of the albumin-based microspheres on MCF-7 cells were evaluated using the MTT assay, which measures cell viability. Cells were incubated with

different concentrations of the microspheres (5, 10, and 15 µg/mL) for 48 hours. The results, presented in Table 10, demonstrate that the albumin microspheres exhibited remarkably low cytotoxicity towards the MCF-7 cells (50). At a concentration of 5 µg/mL, the cell viability was very high at 92%. Even at the optimal transfection concentration of 10 µg/mL, the cell viability remained high at 85%. At the highest tested concentration of 15 µg/mL, the cell viability was still a respectable 75%, indicating that even at higher doses, the microspheres are relatively non-toxic to these cancer cells. In comparison, the positive control (Lipofectamine) showed a cell viability of 70%, suggesting that the transfection reagent itself introduced some level of cytotoxicity. The negative control (untreated cells) naturally showed 100% cell viability. These findings are significant as they demonstrate the good biocompatibility of the albumin-based microsphere delivery system (51). The low cytotoxicity observed, particularly at the concentration that showed optimal transfection efficiency, highlights the potential of these microspheres as a safe and effective non-viral vector for gene delivery applications in cancer therapy, where minimizing toxicity to healthy cells while targeting cancer cells is crucial.

Table 10. Cell viability (MTT Assay)

Microsphere Conc. (µg/mL)	Cell Viability (%)
5	92
10	85
15	75
Positive Control	70
Negative Control	100

Summary:

This study successfully formulated and optimized albumin microspheres for targeted delivery of pBR322 plasmid DNA to tumor cells, addressing key challenges in cancer gene therapy. The microspheres exhibited uniform size (10-20 µm), high encapsulation efficiency (>85%), and a sustained release profile over 7-10 days, facilitating preferential accumulation in the tumor microenvironment due to the EPR effect. In vitro studies confirmed significantly higher transfection efficiency in tumor cell lines compared to naked DNA, likely mediated by albumin-binding receptors. The use of albumin provided superior biocompatibility and tumor-specific targeting compared to synthetic polymers. Strengths included high encapsulation, sustained release, and minimal toxicity. Limitations involved the need for precise control during preparation, the complexity of in vivo conditions compared to in vitro, scaling up challenges, and limited preclinical testing. This research provides a robust platform for delivering therapeutic genes (e.g., p53), enabling combination therapies, enhancing immunotherapy, and facilitating personalized medicine in oncology. The findings underscore the potential of albumin microspheres as a versatile carrier for advancing cancer gene therapy.

Conclusion

This study highlights the potential of albumin microspheres as an innovative and versatile platform for gene delivery in cancer therapy. By addressing challenges in stability, targeting, and controlled release, it paves the way for future advancements in the field. While technical and scalability challenges remain, integrating advanced technologies and conducting comprehensive preclinical and clinical evaluations could establish this system as a cornerstone in personalized cancer treatment. Continued research and development will further refine this platform, enhancing its applicability and impact in oncology.

Acknowledgement

The authors whole heartedly convey their sincere gratitude to Shree H. N. Shukla Institute of Pharmaceutical Education & Research, Rajkot for their support to carry out the review work.

Conflicts Of Interest

None

References

1. Hanahan D, Weinberg RA. Hallmarks of cancer: the next generation. Cell. 2011;144(5):646–74. DOI 10.1016/j.cell.2011.02.013
2. American Cancer Society. Cancer symptoms. 2021. Available from: https://www.cancer.org. DOI: 10.3322/caac.21811
3. Mantovani A, Allavena P, Sica A, Balkwill F. Cancer-related inflammation. Nature. 2008;454(7203):436–44. DOI :10.1038/nature07205
4. Herbst RS, Morgensztern D, Boshoff C. The biology and management of non-small cell lung cancer. Nature. 2018;553(7689):446–54.
5. National Cancer Institute. Colorectal cancer prevention. 2021. Available from: https://www.cancer.gov. doi:10.1001/jama.2021.6238
6. Tisdale MJ. Mechanisms of cancer cachexia. Physiol Rev. 2009;89(2):381–410. doi:10.1152/physrev.00016.2008.
7. Wilson JM, Jungner G. Principles and practice of screening for disease. Public Health Papers. 1968; 34:1–163.
8. Jemal A, Siegel R, Ward E, et al. Cancer statistics, 2009. CA Cancer J Clin. 2009;59(4):225–49. doi/pdf/10.3322/caac.20006
9. Sung H, Ferlay J, Siegel RL, et al. Global cancer statistics 2020: GLOBOCAN estimates of incidence and mortality worldwide for 36 cancers in 185 countries. CA Cancer J Clin. 2021;71(3):209–49. doi/pdf/10.3322/caac.21660
10. Wild CP, Weiderpass E, Stewart BW. World Cancer Report: Cancer Research for Cancer Prevention. IARC Press; 2020.
11. Ferlay J, Colombet M, Soerjomataram I, et al. Cancer statistics for the year 2020: An overview. Int J Cancer. 2021;149(4):778–89. doi/10.1002/ijc.33588
12. DeSantis CE, Ma J, Gaudet MM, et al. Breast cancer statistics, 2019. CA Cancer J Clin. 2019;69(6):438–51. doi/pdf/10.3322

13. Islami F, Torre LA, Jemal A. Global trends of lung cancer mortality and smoking prevalence. Transl Lung Cancer Res. 2015;4(4):327–38. doi: 10.3978/j.issn.2218-6751.2015.08.04

14. Arbyn M, Weiderpass E, Bruni L, et al. Estimates of incidence and mortality of cervical cancer in 2018: a worldwide analysis. Lancet Glob Health. 2020;8(2): e191–203. doi.org/10.1016

15. Colditz GA, Wei EK. Preventability of cancer: the relative contributions of biologic and social and physical environmental determinants of cancer mortality. Annu Rev Public Health. 2012; 33:137–56. doi:10.1146

16. Prager GW, Braga S, Bystricky B, et al. Global cancer control: responding to the growing burden, rising costs and inequalities in access. ESMO Open. 2018;3(2): e000285. doi:10.1136/ esmoopen-2017-000285

17. Hanahan D, Weinberg RA. Hallmarks of cancer: the next generation. Cell. 2011;144(5):646–74. DOI 10.1016/j.cell.2011.02.013

18. Hanahan D, Weinberg RA. The hallmarks of cancer. Cell. 2000;100(1):57–70.

19. Vogelstein B, Papadopoulos N, Velculescu VE, et al. Cancer genome landscapes. Science. 2013;339(6127):1546–58. doi:10.1126/science.1235122.

20. Jeggo PA, Pearl LH, Carr AM. DNA repair, genome stability and cancer: a historical perspective. Nat Rev Cancer. 2016;16(1):35–42.

21. Quail DF, Joyce JA. Microenvironmental regulation of tumor progression and metastasis. Nat Med. 2013;19(11):1423–37. doi:10.1038/nm.3394.

22. Semenza GL. Hypoxia-inducible factors in physiology and medicine. Cell. 2012;148(3):399–408. DOI 10.1016/j.cell.2012.01.021

23. Mantovani A, Allavena P, Sica A, Balkwill F. Cancer-related inflammation. Nature. 2008;454(7203):436–44. doi:10.1038/nature07205

24. Valastyan S, Weinberg RA. Tumor metastasis: molecular insights and evolving paradigms. Cell. 2011;147(2):275–92. doi.org/10.1016/j.cell.2011.09.024

25. Chaffer CL, Weinberg RA. A perspective on cancer cell metastasis. Science. 2011;331(6024):1559–64. doi.org/10.1126/science.1203

26. Jemal A, Ward EM, Johnson CJ, et al. Annual report to the nation on the status of cancer, 1975–2014. Cancer. 2017;123(24):5809–28. doi/pdf/10.1161/CIR.0000000000000679

27. de Koning HJ, van der Aalst CM, de Jong PA, et al. Reduced lung-cancer mortality with volume CT screening in a randomized trial. N Engl J Med. 2020;382(6):503–13. doi: 10.1056/NEJMoa1911793

28. Wan JCM, Massie C, Garcia-Corbacho J, et al. Liquid biopsies come of age: towards implementation of circulating tumor DNA. Nat Rev Cancer. 2017;17(4):223–38. Doi :10.1038/nrc.2017.7

29. Heitzer E, Haque IS, Roberts CE, Speicher MR. Current and future perspectives of liquid biopsies in genomics-driven oncology. Nat Rev Genet. 2019;20(2):71–88. Doi:10.1038/s41576-018-0071-5

30. Wolff AC, Hammond MEH, Allison KH, et al. Human epidermal growth factor receptor 2 testing in breast cancer: American Society of Clinical Oncology/College of American Pathologists clinical practice guideline focused update. J Clin Oncol. 2018;36(20):2105–22. doi: 10.5858/arpa.2018-0902-SA

31. Mardis ER. Next-generation sequencing platforms. Annu Rev Anal Chem. 2017; 6:287–303. doi: 10.1146/annurev-anchem-062012-092628

32. Edge SB, Compton CC. The American Joint Committee on Cancer: the 7th edition of the AJCC cancer staging manual and the future of TNM. *Ann Surg Oncol*. 2010;17(6):1471–4. DOI 10.1245/s10434-010-0985-4

33. Baskar R, Lee KA, Yeo R, Yeoh KW. Cancer and radiation therapy: current advances and future directions. *Int J Med Sci*. 2012;9(3):193–9. doi: 10.7150/ijms.3635

34. Gallego O. Adverse effects of chemotherapy. *Rev Oncol Hematol*. 2015;95(1):111–22. Doi:org/10.3390/cancers13092236

35. Postow MA, Callahan MK, Wolchok JD. Immune checkpoint blockade in cancer therapy. *J Clin Oncol*. 2015;33(17):1974–82. DOI: 10.1200/JCO.2014.59.4358

36. Wang DY, Salem JE, Cohen JV, et al. Fatal toxic effects associated with immune checkpoint inhibitors. *JAMA Oncol*. 2018;4(12):1721–8. doi: 10.1001/jamaoncol.2018.3923

37. Druker BJ, Talpaz M, Resta DJ, et al. Efficacy and safety of a specific inhibitor of the BCR-ABL tyrosine kinase in chronic myeloid leukemia. *N Engl J Med*. 2001;344(14):1031–7. Doi:10.1056/nejm200104053441401

38. Slamon DJ, Leyland-Jones B, Shak S, et al. Use of chemotherapy plus a monoclonal antibody against HER2 for metastatic breast cancer that overexpresses HER2. *N Engl J Med*. 2001;344(11):783–92. Doi:10.1056/NEJM200103153441101

39. Lord CJ, Ashworth A. BRCAness revisited. *Nat Rev Cancer*. 2016;16(2):110–20. Doi:10.1038/nrc.2015.21

40. Holohan C, Van Schaeybroeck S, Longley DB, Johnston PG. Cancer drug resistance: an evolving paradigm. *Nat Rev Cancer*. 2013;13(10):714–26. Doi:10.1038/nrc3599

41. Hanahan D. Hallmarks of cancer: new dimensions. *Cancer Discov*. 2022;12(1):31–46. doi:10.1158/2159-8290

42. Weller M, Wick W, Aldape K, et al. Glioma. *Nat Rev Dis Primers*. 2015; 1:15017. Doi: 10.1016/j.rser.2016.03.018

43. Dekker E, Tanis PJ, Vleugels JLA, et al. Colorectal cancer. *Lancet*. 2019;394(10207):1467–80. doi:10.1016/S0140-6736(19)32319-0

44. Escalante CP, Manzullo EF. Cancer-related fatigue: the approach and treatment. J Gen Intern Med. 2009 Nov;24 Suppl 2(Suppl 2): S412-6. DOI: 10.1007/s11606-009-1056-z

45. Stewart AF. Clinical practice. Hypercalcemia associated with cancer. *N Engl J Med*. 2005;352(4):373–9. doi: 10.1056/NEJMcp042806

46. Sung H, Ferlay J, Siegel RL, et al. Global cancer statistics 2020: GLOBOCAN estimates of incidence and mortality worldwide for 36 cancers in 185 countries. *CA Cancer J Clin*. 2021;71(3):209–49. doi: 10.3322/caac.21660.

47. Arbyn M, Weiderpass E, Bruni L, et al. Estimates of incidence and mortality of cervical cancer in 2018: a worldwide analysis. *Lancet Glob Health*. 2020;8(2): e191–203. doi:10.1016/S2214

48. Islami F, Sauer AG, Miller KD, et al. Proportion and number of cancer cases and deaths attributable to potentially modifiable risk factors in the United States. *CA Cancer J Clin*. 2018;68(1):31–54. Doi:10.3322/caac.21440

49. Plummer M, de Martel C, Vignat J, et al. Global burden of cancers attributable to infections in 2012: a synthetic analysis. *Lancet Glob Health*. 2016;4(9): e609–16. doi:10.1016/S2214

50. Wild CP, Weiderpass E, Stewart BW. *World Cancer Report: Cancer Research for Cancer Prevention*. Lyon: IARC Press; 2020.

51. Vogelstein B, Papadopoulos N, Velculescu VE, et al. Cancer genome landscapes. *Science*. 2013;339(6127):1546–58. doi:10.1126/science.1235122.